FOI-R--0755--SE
March 2003
ISSN 1650-1942
Methodology report

Patrik Thorén

Analysis of LFM pulses received by a hydrophone array in shallow water

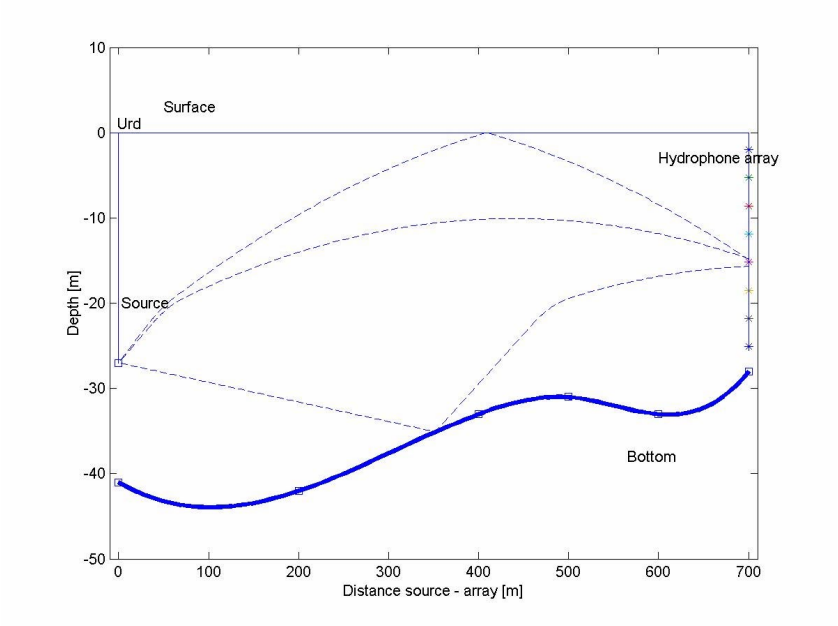

SWEDISH DEFENCE RESEARCH AGENCY
Systems Technology
SE-172 90 Stockholm

FOI-R--0755--SE
March 2003
ISSN 1650-1942
Methodology report

Patrik Thorén

Analysis of LFM pulses received by a hydrophone array in shallow water

Issuing organization	Report number, ISRN	Report type
FOI – Swedish Defence Research Agency Systems Technology 172 90 Stockholm Sweden	FOI-R--0755--SE	Methodology report
	Research area code 4. C4ISR	
	Month year March, 2003	**Project no.** E6051
	Customers code 5. Comissioned Research	
	Sub area code 43. Underwater Sensors	

Author/s (editor/s)	Project manager
Patrik Thorén	Johan Mattsson
	Approved by Eva Dalberg
	Sponsoring agency Swedish Armed Forces
	Scientifically and technically responsible Ilkka Karasalo

Report title (In translation)

Analysis of LFM pulses received by a hydrophone array in shallow water

Abstract (not more than 200 words)

The report presents an analysis of linear FM pulses collected by a vertical 8-hydrophone receiver array in shallow water in the Stockholm archipelago in May 2001. The water depth at the trial site varied from 28 to 42 m, and the pulses were from an omnidirectional source at ranges 50 to 700 m from the receiver array. The source was located at depths 5 and 27 m. The purpose of the experiment was to

(i) identify multiple arrivals in the data and estimate the arrival times, using pulse compression techniques by replica correlation.

(ii) identify the propagation paths of the observed arrivals using sound propagation modelling by ray theory.

(iii) if possible, estimate reflection coefficients at the seabed from bottom-reflected arrivals as a compliment of previous analyses with other techniques at the site.

The data allowed identification of different arrivals in a few cases. For most experimental setups, surface echo arrivals could not be separated from direct arrivals. For the experiments where arrival separation could be done, the arrival time estimates from the sound propagation model fit the data well. Bottom echo arrivals could not be detected, except possible echoes of large bottom objects, located far from the experimental track.

Keywords

Underwater acoustics, sound propagation, ray theory, reflection coefficient

Further bibliographic information	Language English
ISSN 1650-1942	**Pages** 18 p.
	Price acc. to pricelist

Utgivare	Rapportnummer, ISRN	Klassificering
Totalförsvarets Forskningsinstitut – FOI	FOI-R--0755--SE	Metodrapport
Systemteknik	**Forskningsområde**	
172 90 Stockholm	4. Spaning och ledning	
	Månad, år	**Projektnummer**
	Mars 2003	E6051
	Verksamhetsgren	
	5. Uppdragsfinansierad verksamhet	
	Delområde	
	43. Undervattenssensorer	

Författare/redaktör	Projektledare
Patrik Thorén	Johan Mattsson
	Godkänd av
	Eva Dalberg
	Uppdragsgivare/kundbeteckning
	Försvarsmakten
	Tekniskt och/eller vetenskapligt ansvarig
	Ilkka Karasalo

Rapportens titel (i översättning)

Analys av LFM-pulser mottagna av hydrofonarray i grunt vatten

Sammanfattning (högst 200 ord)

Rapporten presenterar en analys av linjära FM-pulser upptagna med en vertikal 8-elements hydrofonarray, på grunt vatten i Stockholms skärgård, maj 2001. Vattendjupet vid försöksområdet varierade mellan 28 och 42 m och pulserna kom från en isotropisk ljudkälla med avstånd 50 till 700 m från mottagaren. Ljudkällan befann sig på 5 och 27 m djup. Syftet med experimentet var att

(i) identifiera multipla ankomster i data och uppskatta ankomsttiderna med hjälp av pulskompressionsteknik med replikakorrelation

(ii) identifiera utbredningsvägar hos de observerade ankomster med hjälp av ljudutbredningsmodellering med strålteori

(iii) om möjligt, uppskatta bottnens reflektionskoefficienter ur ankomster från bottenreflektioner för att komplettera tidigare analyser vid experimentområdet

Identifiering av olika ankomster lyckades i några fall. För de flesta experimenten kunde ej ytekot separeras från den direkta ankomsten. För de experiment där separation lyckades passade de medelst ljudutbredningsmodeller uträknade ankomsttiderna väl med observerade data. Ankomster från botteneko kunde ej detekteras, förutom möjliga ekon från stora objekt, liggande på botten långt från hydrofon-källa-linjen.

Nyckelord

Undervattensakustik, ljudutbredning, strålteori, reflektionskoefficient

Övriga bibliografiska uppgifter	Språk Engelska
ISSN 1650-1942	**Antal sidor:** 18 s.
Distribution enligt missiv	**Pris: Enligt prislista**

FOI1003 Utgåva 11 2002.02 www.signon.se Sign On AB

Contents

1 Introduction 1
2 The experiment 1
3 Methods 3
3.1 Sound ray modelling 3
3.2 Data processing 5
4 Results 9
5 Summary 17
6 Acknowledgements 17
7 References 18

1 Introduction

This report presents an analysis of linear FM pulses (chirps) collected by a vertical 8-hydrophone receiver array in shallow water in the Stockholm archipelago in May 2001. The water depth at the trial site varied from 28 to 42 m, and the pulses were sent from an omnidirectional source at ranges 50 to 700 m from the receiver array. See the introduction in (1) for details on the background to the experiment. The purpose of the experiment was to

(i) identify multiple arrivals in the data and estimate the arrival times, using pulse compression techniques by replica correlation.
(ii) identify the propagation paths of the observed arrivals using sound propagation modelling by ray theory.
(iii) if possible, estimate reflection coefficients at the seabed from bottom-reflected arrivals as a compliment of previous analyses with other techniques at the site.

In section 2 the experiment is outlined briefly. The methods of modelling and data analysis are described in section 3. Results are presented in section 4 and conclusions in section 5.

2 The experiment

The experiment was carried out at the FOI lab site at Djupviken in the Stockholm archipelago, May 7-10, 2001. More detailed technical data on the experiment can be found in (1).

A vertical array of eight equidistant Thomson hydrophones received signals from a transmitter hanging below the test vessel HMS Urd. The hydrophones were positioned 3.3 m apart, with the uppermost 1.8 m below the surface. See Fig. 1 where an example of the setup is presented.

The transmitter, i.e. the Mid Frequency Projector of the Thomson-Marconi Sonar Test System 701 (RAMSE), is an ITC 1007, a piezoelectric ceramic device of spherical design. Its operating frequency range is 2.5 to 25 kHz. The transmitted signals were 0.02 s long FM sweeps (sometimes referred to as “chirps”) at frequencies 5-9 kHz. Theoretically the signal should vary as

$$P=A*\cos(2*\pi*(F1+DF*T/DT)*T)$$

where T is the time, varying from 0 to 0.02 s, DT is the chirp length (0.02 s) and A is the amplitude. F1 is the frequency at the beginning of the chirp, F1+DF is the final frequency (in this case F1=5000 Hz, DF=4000 Hz).

The real transmitted signal will be distorted in various ways, due to e.g. nonlinearity in the transmitting equipment.

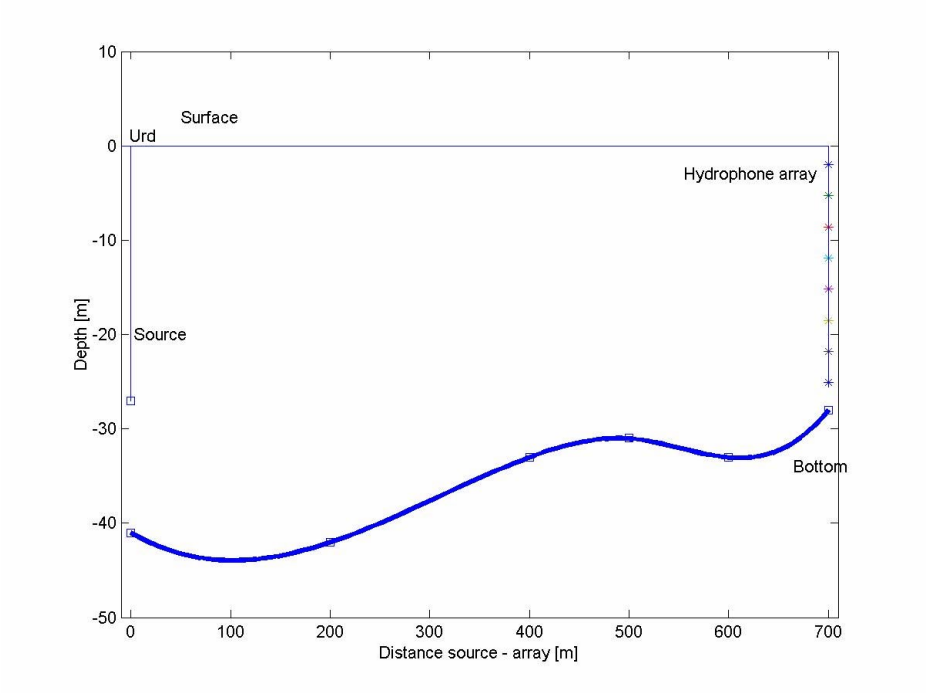

Figure 1. One of the experimental setups. The bottom is modelled with a cubic spline function. The squares at the bottom represents actual measured depths. The source was positioned at a depth of 27 m in this setup, 700 m from the array.

In each experimental setup signals were sent every 5 seconds during two minutes. The chirps were transmitted from two different depths (5 and 27 m) at distances between 50 and 700 m from the array. The same track was used as in (1). The bottom depth at the test track varied between 31 and 42 m and was 28 m at the array. In Fig. 1 the bottom has been interpolated with a spline function between the measured depths (marked with squares).

The sound velocity profile was measured several times during the experiment and varied slightly as seen in (1, Fig 2.1). A simplified piecewise linear velocity profile was used in this work, as shown in Sect. 3.1.

3 Methods

3.1 Sound ray modelling

The arrival times of the signals, registered with the hydrophones, have been compared with modelled arrival times. The sound rays were modelled with MATLAB, using Snell's law (see e.g. 3)

$\cos \Theta_{i+1}/c_{i+1} = \cos \Theta_i/c_i$

where c is the sound velocity in water and Θ is the elevation angle of the sound ray.

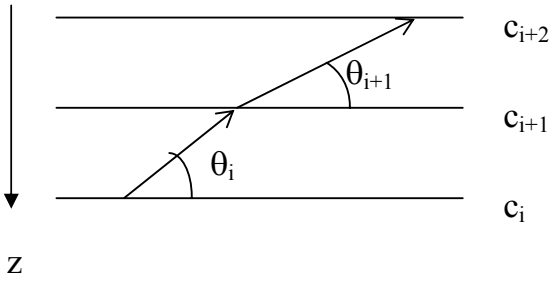

Figure 2. According to Snells law a sound ray propagating through layers with different sound velocity is refracted. Arrows with unfilled heads represent an upward propagating sound ray, z shows depth, c_i is sound velocity at depth i.

An approximate piecewise linear velocity profile from sound velocity measurements during the experiment was used, see Fig. 3 and (1). The effect on changes in arrival times of the echoes, both when changing the velocity profile within the measured values and to a constant value, is smaller than what was measurable in the experiment.

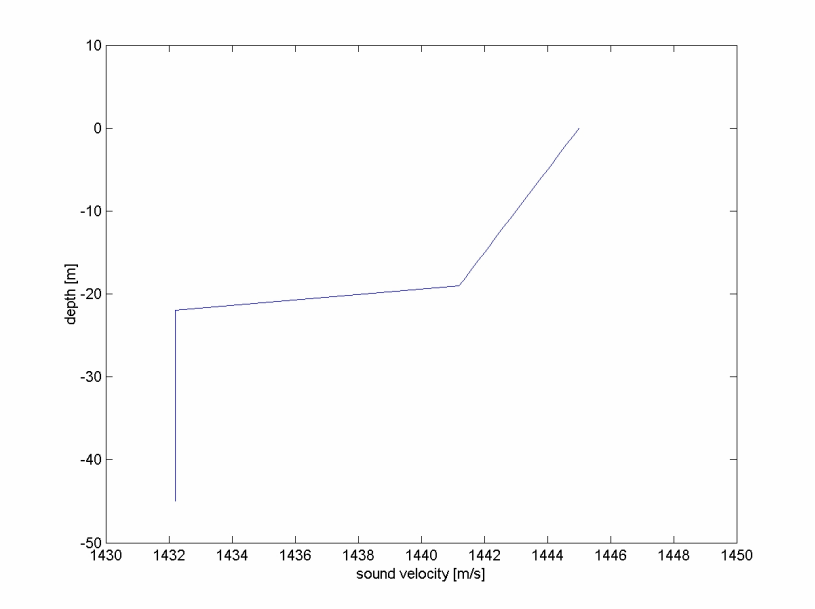

Figure 3. Sound velocity profile for the modelling.

The depth at the source was measured from the test vessel during each setup. This allowed modelling of the depth profile for the test track. The bottom profile between the measurement points was interpolated with a spline function. For the setups with small separations, 200 m or less, the rays were modelled to be reflected as if from a flat bottom, parallel with the surface. The depth does not vary much on those small distances. This means the flat bottom reflection can safely be used in the derivation of arrival times. In Fig. 4 five different rays are plotted, showing the sound path from the source to one of the hydrophones. The three different bottom paths show the ways the bottom reflection has been treated in this investigation. The dotted-dashed line show the path if a constant depth is used (the depth at the source). The dashed line show the path if the bottom is linearly interpolated between the measured depth points. The solid line corresponds to the path when spline interpolation is been used. Shown in Fig. 4 is also the bottom profile interpolated with a cubic spline.

The difference in bottom echo arrival, when using either constant depth or depth spline interpolation for the reflection treatment, is on the order of 0.001 s or smaller. The upper difference limit applies to large separations. For smaller separations the time difference becomes much smaller, due to the almost flat bottom. For the sound ray propagation constant bottom depth has been used for the closer setups – distance between source and array 200 m or shorter. For the more separated setups, spline interpolation has been used.

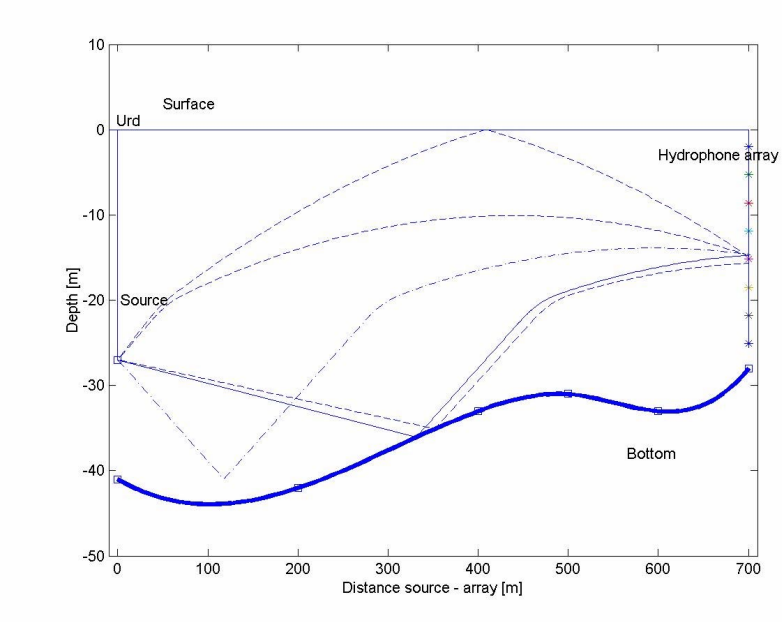

Figure 4. Example of experiment setup and ray paths to the fifth hydrophone in the array. Three different ways to treat the bottom bounce are shown.

3.2 Data processing

The experimental data was analysed with MATLAB. At each source location 0.02 s long LFM pulses were emitted with pulse repetition frequency 0.2 Hz during two minutes. This would theoretically give about 25 pulses per hydrophone and setup. For each setup the first ten useable pulses were identified, filtered and correlated with a synthetic signal. The reason for using only ten pulses was that for some setups (especially those with large separations between source and array) only ten pulses could be identified in the noise. By using the same amount of data for each setup, data comparisons between setups and between hydrophones would presumably be easier. The pulses were identified both by listening to the signal (using the MATLAB SOUND routine) and, for more noisy data, by visual detection after filtering and correlation with a synthetic chirp.

The filtering was done with FFT-processing of a two-second time-window enclosing each pulse. By comparing the signal in the frequency domain with a FFT transform of a synthetic chirp, the noise frequencies were identified. The frequency regions marked “s” in the FFT-windows of Fig. 5 corresponds to the signal. The FFT-transformed signal elements corresponding to the noise (outside the “s”-regions) frequencies were set to zero and transformed back from the frequency domain. After inverse FFT transformation the pulse is, as seen, cleaned from low frequency ambient noise.

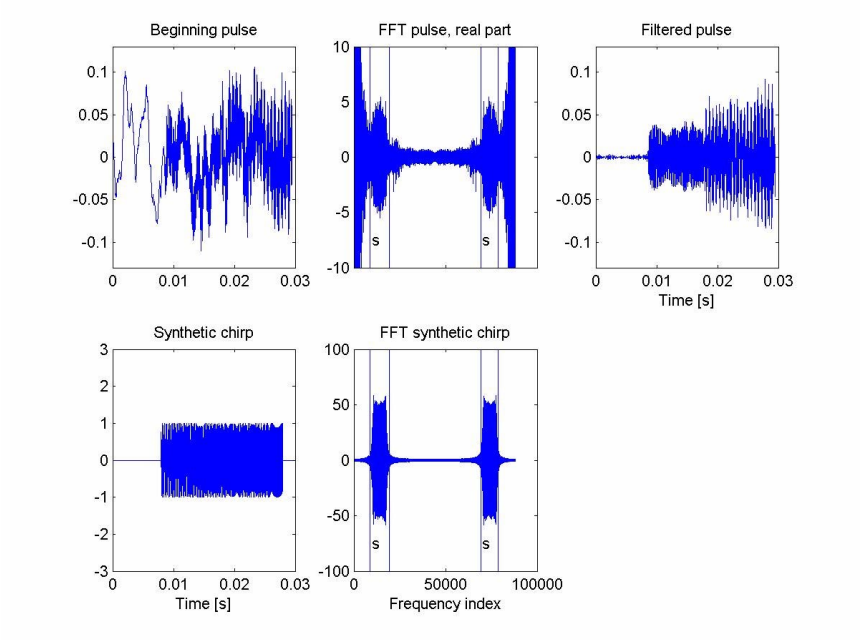

Figure 5. Low frequency noise removal. Regions in FFT plots recognized as pure signal marked with "s".

The synthetic signal was a 0.02 s linear frequency sweep from 5-9 kHz produced with the MATLAB CHIRP routine. No experimental setups rendered a time difference between the direct path and surface echo longer than the chirp length. The ray path models produced time differences between direct path and surface echo varying from virtually 0.00 s to 0.017 s. The latter time corresponds to one single setup with 50 m separation. All other setups produced time differences smaller than 0.01 s. Thus, for direct comparison between synthetic and real signal, only about the first two thirds of the chirp could be used (see example of blurring start about 0.01 s after beginning of *Filtered pulse* in Fig. 5). Fig. 6 shows that the frequency of the synthetic signal well matches that of the observed signal until surface echo interference begins. The pulse studied in Fig. 5 was produced in the extreme case setup with 50 m separation.

It thus appears that the chirps produced by the transmitting equipment are well simulated by the synthetic chirp, as far as they are comparable. The latter will then not incur errors due to inaccurate frequencies when used for the correlation analysis.

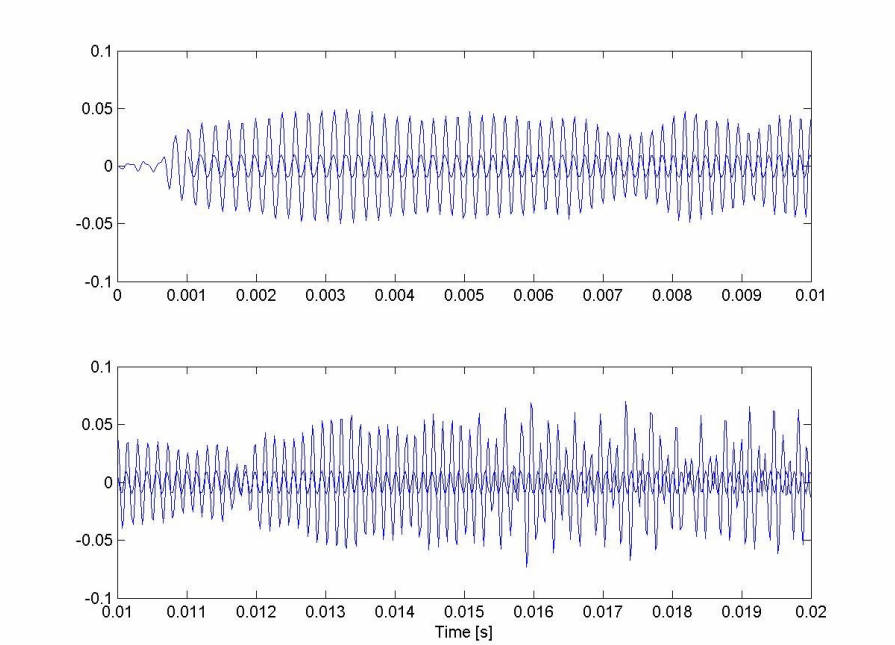

Figure 6. Example of filtered chirp with synthetic chirp (small amplitude) overplotted.

After filtering, the pulses were correlated with the synthetic chirp. The result of such a correlation for one setup and one pulse is shown in Fig. 7.

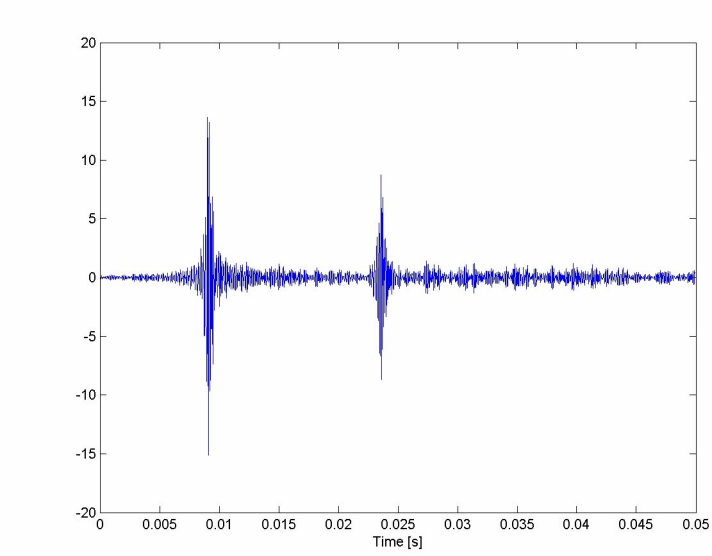

Figure 7. Observed signal correlated with synthetic chirp. Hydrophone closest to bottom, source 50 away at depth of 27 m. First arrival corresponds to the direct path. The second arrival is a surface echo.

To increase the signal-to-noise-ratio the absolute values of the ten first usable correlated pulses in each setup were added. The positions of the pulses were determined by plotting each correlated pulse and then finding the maximum or minimum of a prominent pulse feature by eye. The precision of this method is better than one wavelength for the correlated pulse. Since

the pulse-to-pulse variation in arrival times between different echoes may differ more than half a wavelength there is no need for better precision than that. The result of a correlated pulse addition can be seen in Fig. 8, where the addition has been done for all the hydrophones.

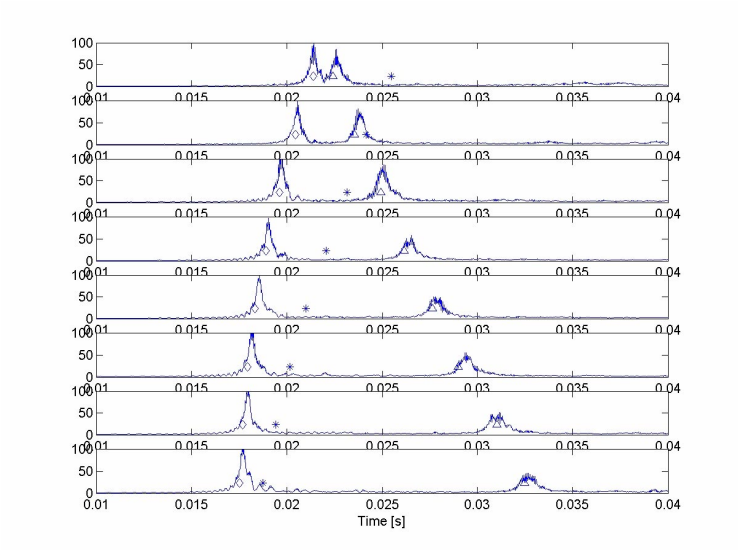

Figure 8. Sum of absolute values of ten pulses for hydrophone 1-8 in the array. Source 50 m from array, at depth of 27 m. Positions for theoretical arrival times (compared to the direct path) are marked with diamonds (direct), stars (bottom echo) and triangles (surface echo).

As seen in Fig. 8 the arrival times of the direct pulse and the surface echo line up well with the times of the ray model. The bottom echoes are however not visible at the positions suggested by the ray model. Apparently the reflection at the bottom is too weak.

4 Results

In figures 9–19 the resulting processed (filtered, correlated, time-aligned and added) pulses are plotted for the different source positions. The time zero points are arbitrarily chosen. The calculated arrival times for direct path (triangles), surface echo (diamonds) and bottom echo (stars) are also plotted.

It appears that pulses arriving along the direct path and surface echo paths are always observable, except at hydrophones positioned in the sound shadow zone. Close inspection reveals that the proposed (when resolved, see below) surface echoes have inverted signs compared to the sign of the proposed direct path signal. For setups with the source close to the surface it is difficult to distinguish between direct path pulse and surface echo pulse due to the very close arrival times. In Fig. 15 (source at 5 m depth), where the source-array distance is 130 m, the direct pulse and the surface echo appear to be separated for the lowest four hydrophones only. For larger distances, arrival separation cannot be made. For setups with source set deep (27 m) the direct and surface arrivals can be separated for all hydrophones up to 200 m (Fig. 11). At larger distances those arrivals merge and become indistuingishable.

The bottom echo is difficult to observe in the data. A signal, lagging behind the suggested bottom arrival time with 0.01 s or more and smeared out in a reverbationlike manner, is visible in some spectra. By changing the model depth with 5 - 10 m or more, the model bottom echo arrival time can be fitted to the observed feature, but such a large uncertainty in the depth measurement is unlikely. Reasonable uncertainties in the velocity profile cannot either cause the discrepancy. It is therefore suggested that the observed smeared out echoes are not connected to the bottom reflected ray paths, rather to bottom reverbation from off-track areas.

For some cases (e.g. Fig. 11) a more peaked signal with a varying time lag is visible. These echoes may be reflections from large underwater objects on the bottom, beside the test track. The source is omnidirectional, which allows echoes far from the track. One way to find the location of the objects is to plot the possible positions on the bottom for echoes to each hydrophone according to the observed time lag. For the lagging signal in e.g. Fig. 11 it is indeed found that an underwater object would give consistent bottom echoes when positioned 180 m from the source and 25 m from the test track. In Fig. 20 the ellipses plotted corresponds to the time lag between direct pulse and the observed echo. Each ellipse represents possible positions of an object on the seafloor consistent with the observed time lag. The area where all ellipses intersect is suggested to contain a bottom object. The position of an object in another setup found in the same way is shown in Fig. 21.

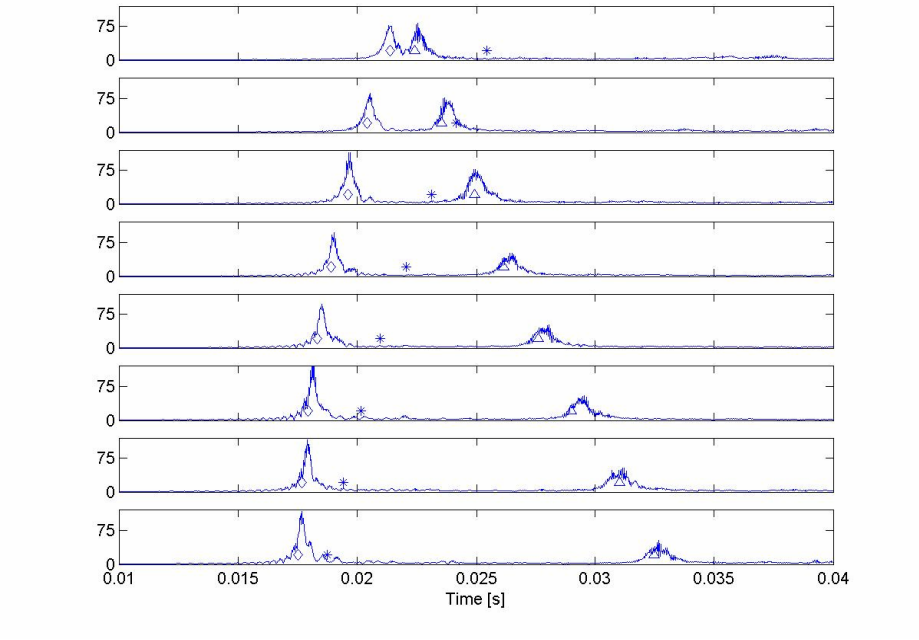

Figure 9. Pulse 13, separation 50 m, source at depth 27 m.

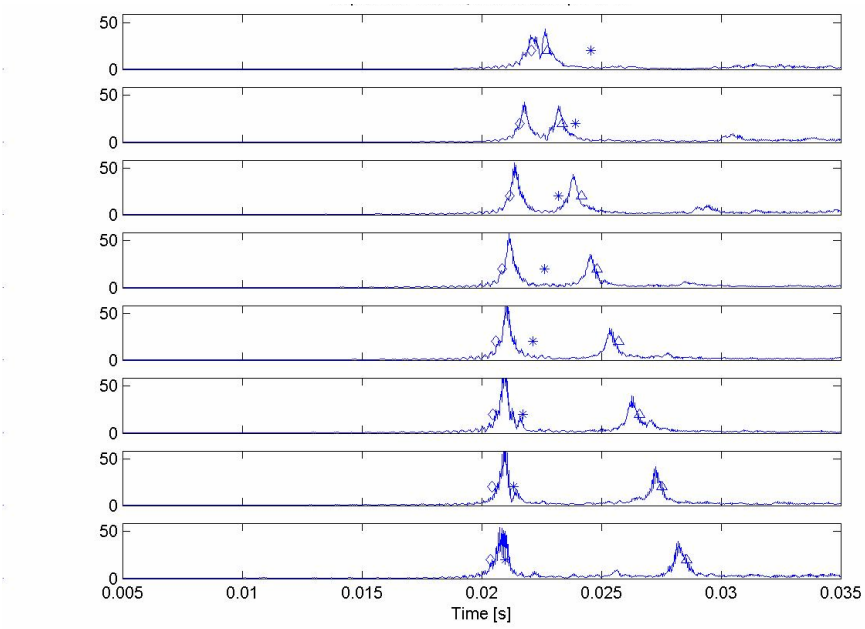

Figure 10. Pulse 12, separation 100 m, source at depth 27 m.

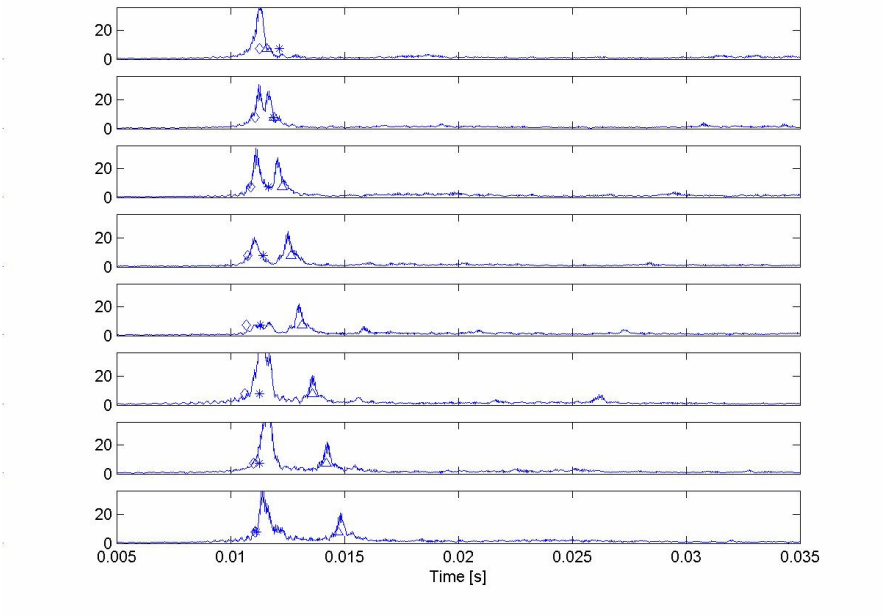

Figure 11. Pulse 11, separation 200 m, source at depth 27 m.

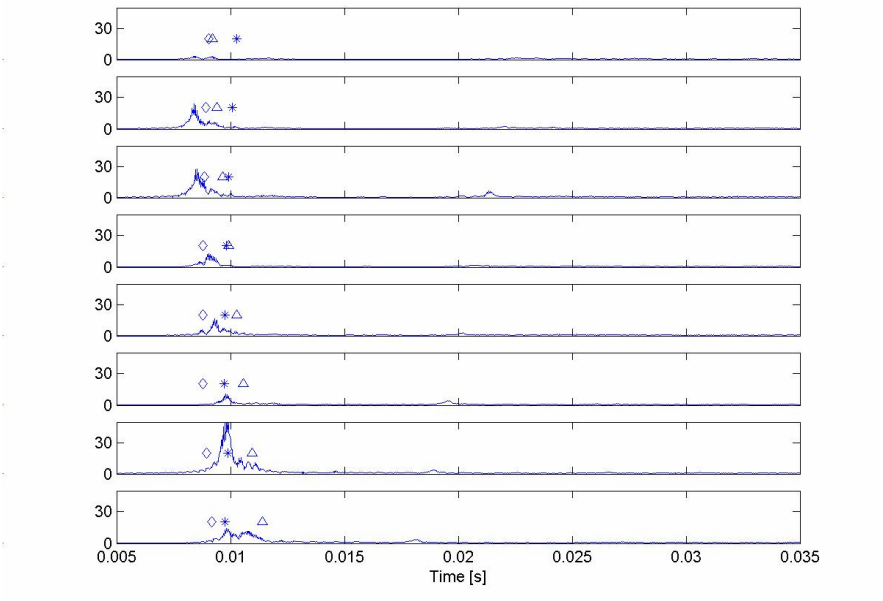

Figure 12. Pulse 10, separation 300 m, source at depth 27 m.

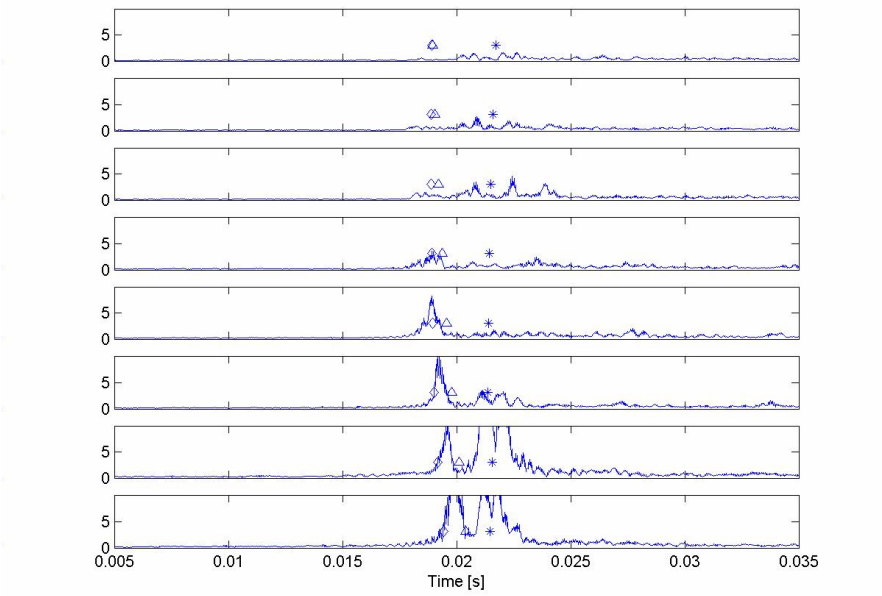

Figure 13. Pulse 9, separation 500 m, source at depth 27 m.

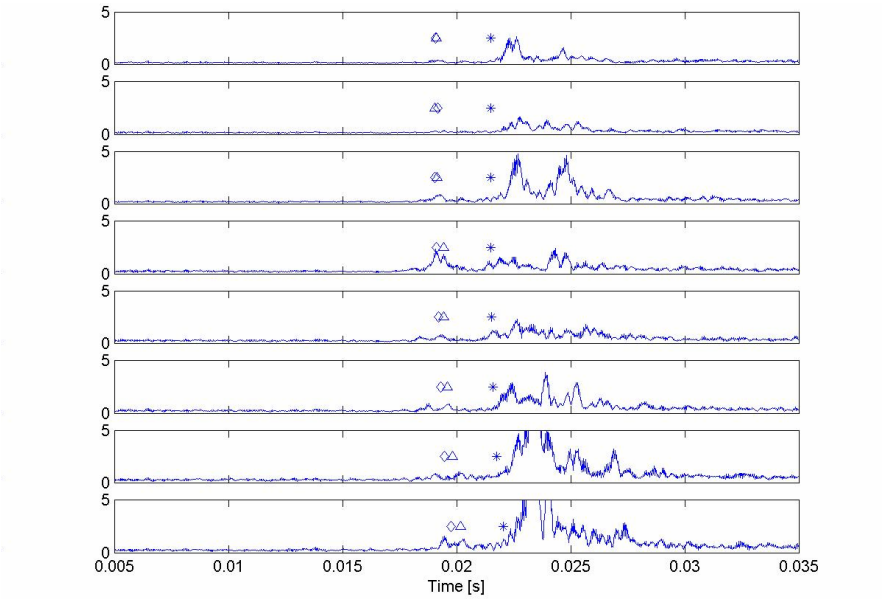

Figure 14. Pulse 8, separation 700 m, source at depth 27 m.

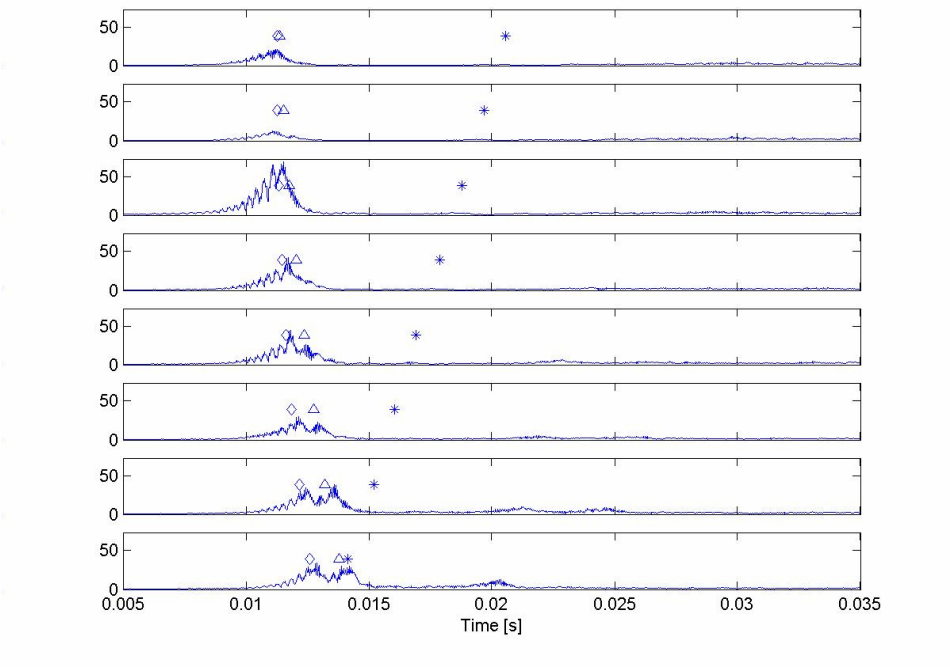

Figure 15. Pulse 3, separation 130 m, source at depth 5 m.

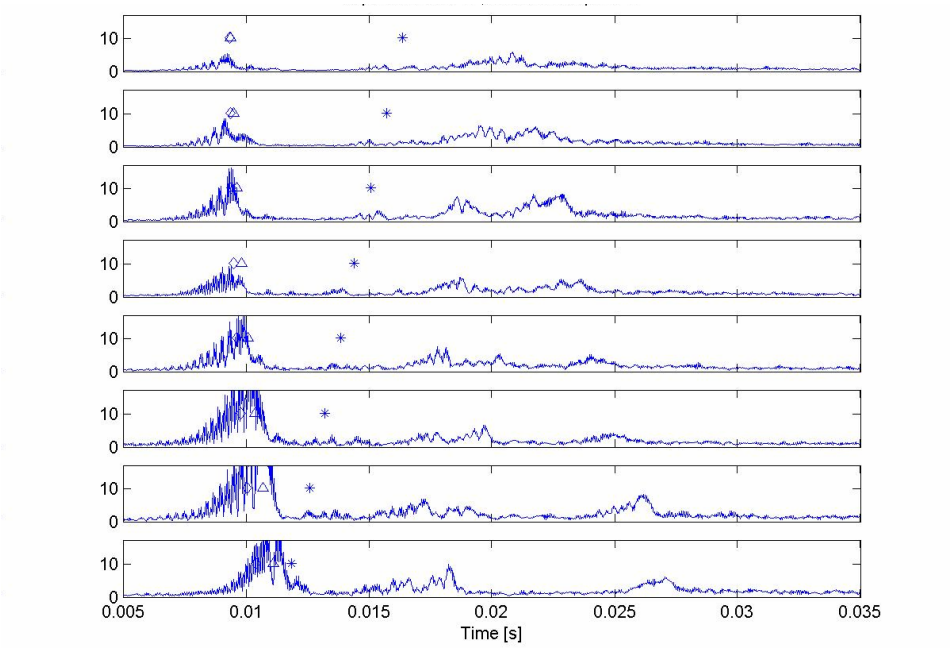

Figure 16. Pulse 4, separation 200 m, source at depth 5 m.

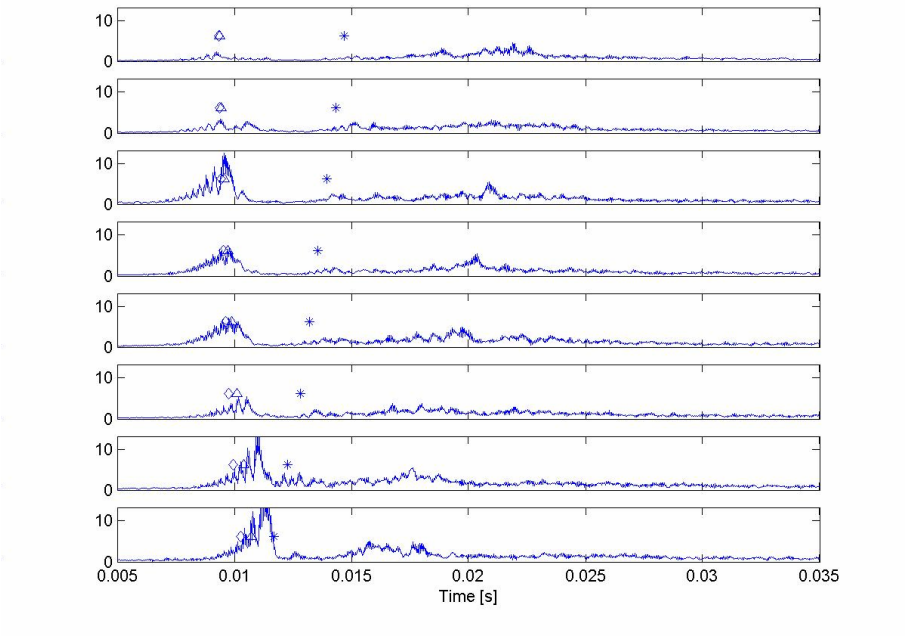

Figure 17. Pulse 5, separation 300 m, source at depth 5 m.

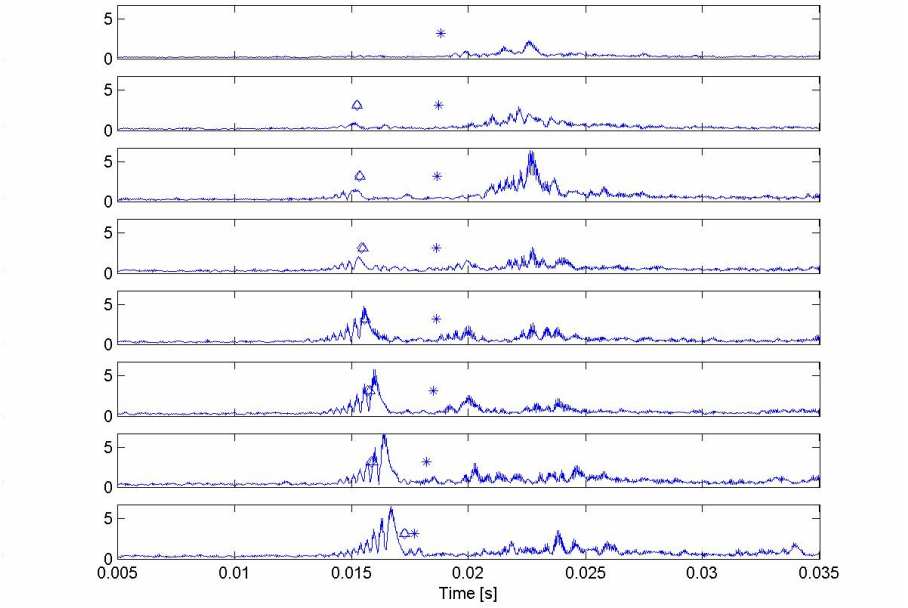

Figure 18. Pulse 6, separation 500 m, source at depth 5 m.

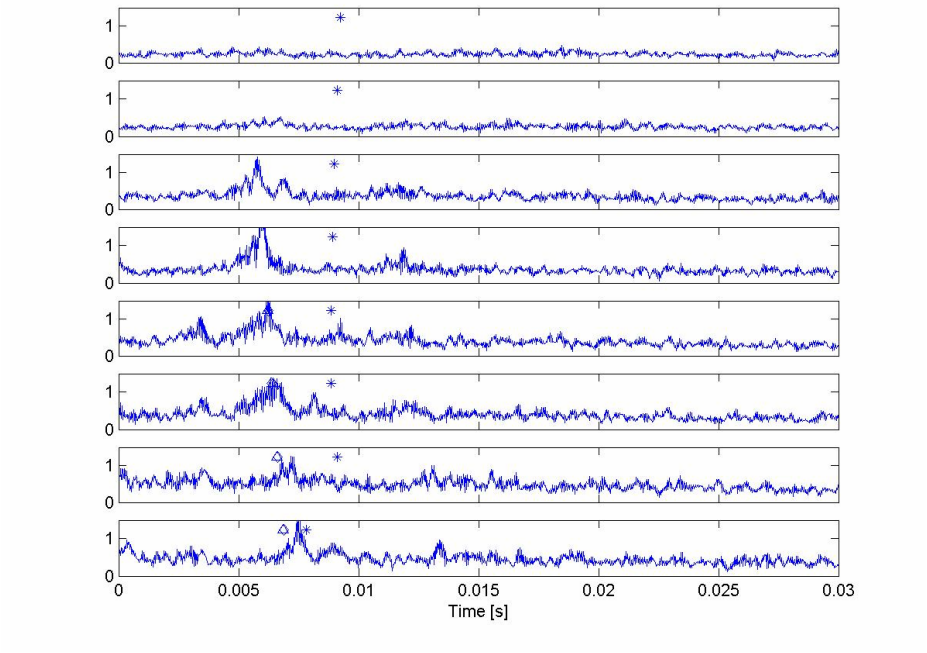

Figure 19. Pulse 7, separation 700 m, source at depth 5 m.

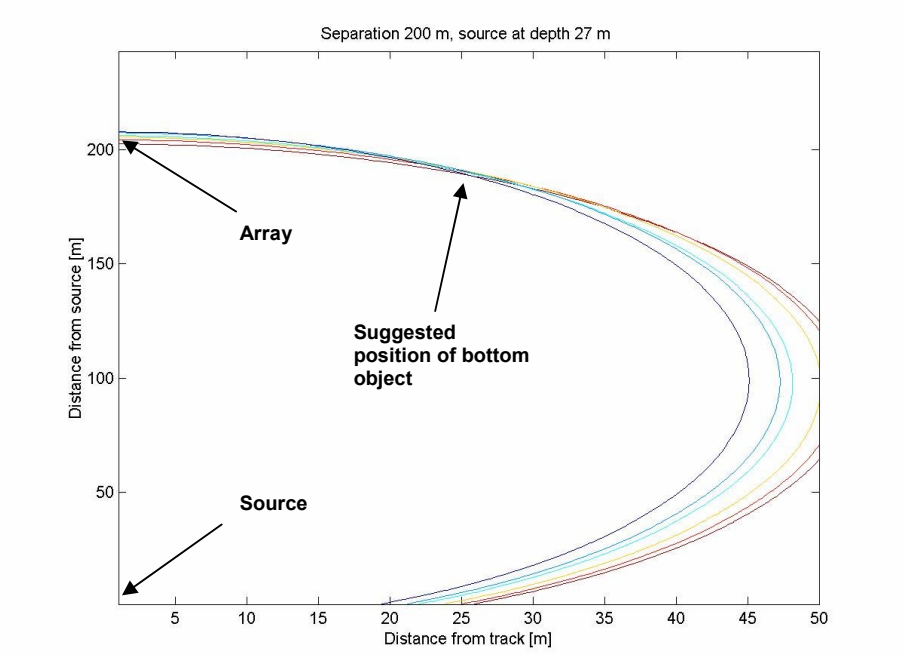

Figure 20. Ellipses corresponding to time lags between observed direct pulse and echo. Each ellipse represents possible positions of a bottom object consistent with the time lag observed by one hydrophone. For two hydrophones no echo was observed. The area where the ellipses intercect indicates the position of the object to be 180 m from the source, +/- 25 m from the test track.

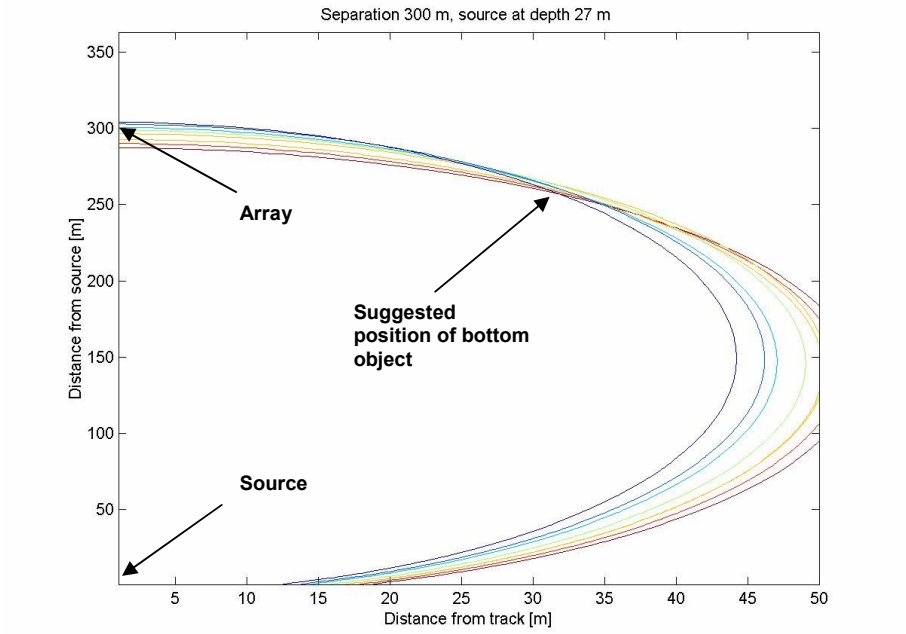

Figure 21. Possible positions of bottom object, measured with all eight hydrophones. See Fig. 6 for information. Bottom object position: 260 m from source, +/- 30 m from test track.

The amplitudes of the direct and surface echo pulses have been compared for some clearly separated arrivals. This was done by direct integration of the pixel values over the correlated

pulses and comparison between the derived values for different pulses and hydrophones. The direct path and surface echo amplitudes appear to be similar. There are no clear signs of weakening of the surface echo due to absorption loss. The spectra are noisy and do not allow pulse energy content measurements with high accuracy within the scope of this report.

A delayed reverbation is the only observable sign of the bottom (except for the suggested objects), visible for some of the setups. Since the direct bottom echoes are not observed, only an upper limit can be established for the bottom reflection coefficient. With the same correlated pulse energy integration as described above at least 80 % of the signal energy is transmitted into the bottom. It is however not unlikely that what has been integrated over is noise only and then the energy reflected must be even smaller. Different measurements of the bottom density and sound velocity close to the test site indicate impedance between $1.6 * 10^6$ kg/m^2s (4) to $2.2 * 10^6$ kg/m^2s (5). Inversion of seabed parameters along the test track (1) suggested bottom impedances between $2.2 * 10^6$ kg/m^2s and $3.3 * 10^6$ kg/m^2s**.** A weak impedance contrast between the bottom and the seawater (impedance ca $1.5 * 10^6$ kg/m^2s) could explain the small bottom reflection (2). A very rough bottom could also scatter the bottom directed signals and explain the lagging reverbation but (4) reported roughness of only a few centimeters close to the trial area.

5 Summary

The purpose of the experiment was to identify multiple arrivals in the data and estimate the arrival times, to identify the propagation paths of the observed arrivals using sound propagation modelling, and to estimate reflection coefficients at the seabed from bottom-reflected arrivals.

In a few setups (small separation between source and array and/or source close to the bottom) the multiple arrivals of direct and surface paths could be identified. At separations larger than 200 m the arrivals merge and become indistuingishable. The bottom echoes are difficult to observe in the data, except for delayed reverbation and a number of possible underwater object echoes (see below).

The propagation paths of the direct and surface paths have been calculated with a sound propagation model, and the corresponding modelled arrival times fit well with the observed data. The data for bottom echoes are however too weak in all experimental setups to confirm the modelled propagation bottom echo paths. Echoes from a number of possible underwater objects were observed in the data. The locations of these objects were calculated (with the sound propagation model) to be 25-30 m from the test track.

Due to the weak signal the of the bottom echo, the reflection coefficient of the sea bed could not be established. The weak bottom echo suggests a small impedance contrast between the sea water and the sea bed, or a very rough bottom.

6 Acknowledgements

I thank Ilkka Karasalo for guiding and useful suggestions on the manuscript. Brodd Leif Andersson, Sven Ivansson, Per Morén and Elias Parastases are thanked for assistance during the analysis.

7 References

(1) Leif Abrahamsson & Brodd Leif Andersson. Inversion of seabed parameters in the Stockholm archipelago. FOI report R – 0300 – SE, 2001.
(2) Urick, Robert J. Principles of Underwater Sound, 3rd edition, 1983.
(3) Jens M. Hovem. Marin Akustikk, kompendium.
(4) Bjarte Berntsen, Ilkka Karasalo, Mika Levonen, Per Morén Per & Viggo Westerlin**.** Seabed characterization in the Baltic with SIROB and FARIM methods, FOA-R--99-01237-409—SE, 1999.
(5) Bjarte Berntsen, "Model-based estimation of seafloor parameters by use of acoustic back scattering", PhD thesis, 2001.